Journal of New Technology and Materials (JNTM)
J. New Technol. Mater.
Vol. 10, N°02 (2020)64-69

OEB Univ. Publish. Co.

Study of New Antimony Phosphate Glasses

F. Zohra Agti[a, b *], M. Toufik Soltani[a], Luis F. Santos[b], A. Messaoudi[c] and D. De Ligny[d]

[a]*Laboratory of Physics of Photonics and Multifunctional Nanomaterials, University Mohamed Khieder of Biskra, Biskra, BP 145, RP, 07000, Algeria*
[b] *Department of Chemical Engineering and CQE, Av. RoviscoPais 1, Instituto Superior Técnico, Technical University of Lisbon, Lisboa, 1049-001, Portugal*
[c]*Research Laboratory in Civil Engineering, Biskra, University Mohamed Khieder of Biskra, Biskra, Bp145, 07000, Algeria*
[d]*Department of Materials Science and Engineering, Institute of Glass and Ceramics, University of Erlangen- Nuremberg, Erlangen, 91058, Germany*
*Corresponding author, email: fatima.agti@univ-biskra.dz

Received date: June 10, 2020 ; revised date: Nov. 07, 2020 ; accepted date: Nov. 09, 2020

Abstract

Crystallization kinetic studies of ternary antimonite glasses within the 60 Sb_2O_3-(40-x) $NaPO_3$-xWO_3 system x= (5, 15) were prepared using the melt quenching technique were performed by non-isothermal methods using differential scanning calorimetric (DSC) its measurements showed glasses a very stable with the addition of WO_3. The kinetic parameters Ea and n by applying Ozawa and Chen methods were found to be in good agreement with each other the values of crystallization activation energy were calculated in the range of 49, 30 Kcal.mol^{-1} (Chen) and 52, 33Kcal.mol^{-1} (Ozawa) and Avrami constant, n_{moy}(SN5W)=2.05, n_{moy}(15W)= 2,01 correspond decreasing nucleation rate. The evolution of hardness appears increases linearly versus tungsten content in the glasses; the hardness is close from 325 to 425. This study could open new avenues of research for ternary antimony-based glasses for applications in nonlinear properties.

Keywords: Sb_2O_3, Crystallization, Differential scanning calorimetric, Tungsten, Activation energy.

1. Introduction

Antimony phosphate glasses and tungsten ion containing glasses exhibit interesting properties for applications of non-linear properties [1] in fibres and laser generation, low melting temperature, and chemical stability ([2],[3]).

Antimony Oxide glasses have properties like a large transmission window from UV to IR [4], high mechanical properties. And up-conversion emissions are usually strong [5]. On the other hand, studied of binary systems based on antimony oxide with tungsten and with phosphate confirmed increase of the glass transition temperature and thermal stability against crystallization that depends on the crystalline growth of germs and germination or nucleation and depend of deferent concentration of $NaPO_3$ and WO_3 in the composition ([5], [6]).

The crystallization process develops from germs (or nuclei) or heterogeneous nucleation of impurities from the surface, at higher temperatures, these germs grows and leads to the formation of crystalline particles. New materials developed with help senarmontite antimony-based glasses at the mechanism of growth [7].

We used Chen and Ozawa from many methods of analysis has been proposed. So the present work is to study of crystallization kinetics on

Two different concentrations tungsten oxide in the antimony phosphate glasses.

2. Experimental procedure

The synthesis of the glasses is carried out in the air, in a silica tube, from a calculated mixture of initial components, by direct reaction and melting at temperature close to 1000 ° C. The mixture is completely melted after two minutes, the bath is then homogenized for three minutes, and this time must remain limited due to the tendency to vaporize Sb_2O_3 and $NaPO_3$ whose melting temperatures are 656 ° C and 628 ° C respectively. During the exploration of the vitreous state, the molten mixture is poured on a metal plate at room temperature and flattened with a second piece metallic when you want to increase the quenching speed. The glass solidifies with great mechanical fragility due to the residual internal stresses due to quenching. If the tempering is too slow, we observe a crystallization of the glass from its surface in contact with the air, to obtain relatively bulky glass masses capable of to be cut and polished, the molten bath is poured into a brass mold previously heated to a temperature close to Tg (glass transition temperature of the glass considered). An annealing cycle is then carried out: the glass is brought to a temperature T close to Tg (T

≈ Tg-10 ° C) for 6 hours then leave to cool slowly to the ambient.

The thermal characterization was carried out by the differential calorimetric by scanning; Samples are placed in aluminum crucibles, by running non-isothermal at different heating rates.

Vickers hardness was measured using a Duramin20 (Struers) micro hardness tester at indentation loads from 1.961N to 20 N, HV 0.2 and a load of 200 g is applied for a time of 20 seconds, for the same sample. At each load at least four indents were spaced at about 38, 97 µm intervals then the mean was calculated, an average value was calculated from five successive measurements made for each sample. The relative error on the micro hardness values is mainly due to the error on the reading of the values of the diagonals.

3. Results

3.1 Non-isothermal crystallization method

The theoretical basis for interpreting transformation kinetics, the study of crystallization of glasses $60Sb_2O_3$-35 $NaPO_3$-$5WO_3$, $60Sb_2O_3$-25 $NaPO_3$-$15WO_3$ systems the activation energy is none other than the slope Ea/R in absolute value of the line. The Avrami coefficient is obtained by measuring the crystallized fraction at a given temperature but with different heating laws.

The Avrami Exponent Determination n is based on the Avrami equation (1) [8].

$$x = 1 - \exp[-(kt)^n] \quad (1)$$

The temperature is thus defined by the equation 2:

$$T = To + \alpha t \quad (2)$$

T: Temperature at moment t (°K).
To: The temperature from which the heating rate (°K) was applied.
α: Heating law (°K/min).

The temperature of the sample varies linearly as a function of time, the transformations made by the sample being recorded as a function of temperature. Determination of the activation energy Ea is based on the evolution of the peak position referring to equation (2) and taking twice the Nepalese logarithm, it becomes equation trios [9]:

$$\ln(-\ln(1-x)) = n\ln k(T - To) - n\ln(\alpha) \quad (3)$$

If T is fixed the term n ln k (T-To) will be constant.
The calculation of the Avrami coefficient n is obtained from the slope of the line ln(α)=f (ln (-ln (1-x))) [10].
Chen [11] and Ozawa equations [12] are used, which derive from the general law formulated by Kemeny and Sestak [9] and which allow the calculation of the activation energy Ea (equations 4, 5).

$$\text{Ozawa} \quad \ln(\alpha) = -\frac{Ea}{R}.Tp + \text{constant} \quad (4)$$

$$\text{Chen} \quad \ln(Tp^2/\alpha) = Ea/R.Tp + \text{constant} \quad (5)$$

In both cases, the calculation of the activation energy follows the general equation 6:

$$\text{Ln}(Tp^m/\alpha) = Ea/R.T + cte \quad (6)$$

α : Law of heating.
Tp: Temperature of peak crystallization.
Ea: The activation energy.
R: Perfect gas constant (J/K. Mol)
T: Temperature (°C).
The exponent m is equal to 0 in the relation of Chen, and to 2 for Ozawa. The value of Ea/R is deduced from the slope of the line drawn [13].

3.2. Thermal characterization

Figures 1 and 2 show the thermal analysis curves by differential calorimetric by scanning (DSC) of 60 Sb_2O_3-35 $NaPO_3$- $5WO_3$ and 60 Sb_2O_3-25 $NaPO_3$- $15WO_3$ by running non-isothermal at different heating rates (5,8,10,15,20) and (6,8,10,12).

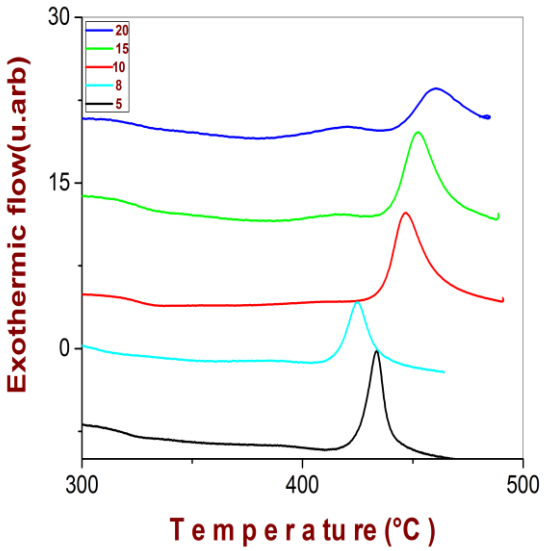

Figure 1. DSC Curves of 60 Sb_2O_3-35 $NaPO_3$- $5WO_3$ vitreous to different heating laws.

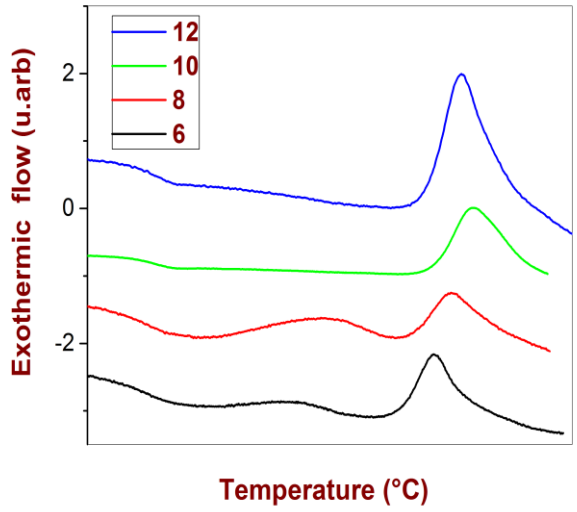

Figure 2. DSC Curves of 60 Sb_2O_3-25 $NaPO_3$-15WO_3vitreous to different heating laws.

3.3. Determination of activation energy (Ea) and Avrami coefficient (n)

Done determine the parameter of the deviation the apparent activation energy "Ea" of two more stable compositions, the heating laws giving the most coverage of the different peaks of crystallization were chosen to conduct this non-isothermal study. With the relations of Chen, and Ozawa, it is possible to follow the displacement of the crystallization peak according to the law of heating; the table1 shows the calculations of the parameters and the figures 3 and 4 show determination results of activation energy by methods Chen and Ozawa for ternary glass.

Table 1: Calculations of the parameters of the non isothermal method for 60 Sb_2O_3- 35 $NaPO_3$- 5 WO_3, 60 Sb_2O_3-25$NaPO_3$- 15WO_3.

Composition	α (°K/min)	ln (α)	Tp (°k)	10^3/Tp ($°K^{-1}$)	Ln(Tp^2/α)
SNW 5	20	2,99573	733,53	1,36327	10,20000
	15	2,70805	724,50	1,38026	10,46291
	10	2,30259	719,60	1.38966	10,85481
	8	2,07944	712,60	1,40331	11,05831
	5	1.60943	706,50	1,41542	11,51121
SNW 15	12	2,48491	728,09	1.37345	10,69594
	10	2,30259	731,16	1.36769	10,88668
	8	2,07944	723,64	1.38190	11,08915
	6	1,79179	714,99	1.39862	11,35278

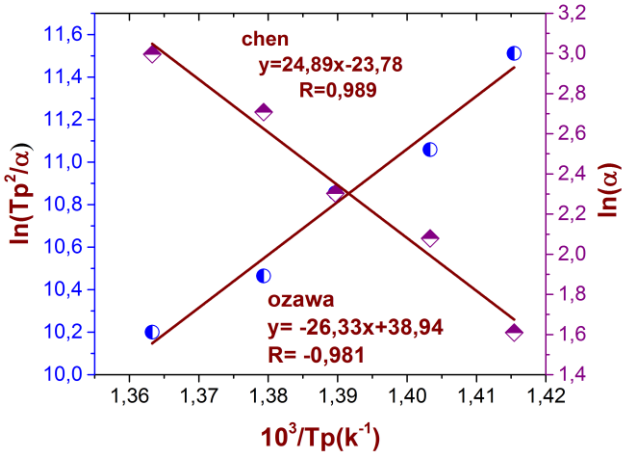

Figure 3. Determination of activation energy by methods Chen and Ozawa for 60 Sb_2O_3-35 $NaPO_3$- 5WO_3glass.

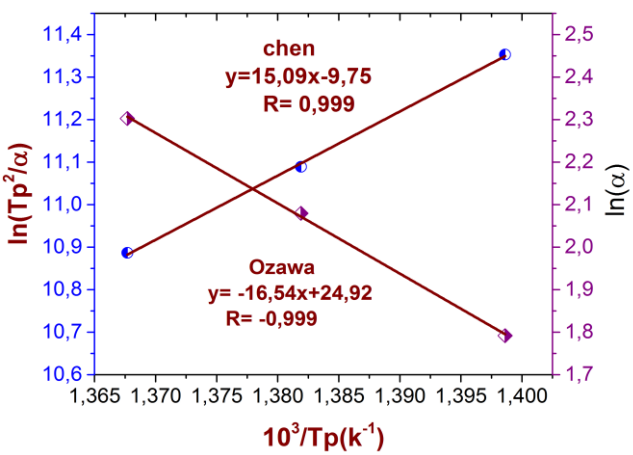

Figure 4. Determination of activation energy by Chen and Ozawa methods for 60 Sb_2O_3-25 $NaPO_3$- 15WO_3glass.

The values of activation energy calculated from the Chen and Ozawa methods grouped in the table 2.

Table 2: Activation energy

Composition	Activation Energy [Kcal.mol^{-1}]	
	Chen	Ozawa
SNW 5	49,44±4,362	52,29±4,356
SNW 15	30,44 ±0,88	33,36 ±0,87

In the $60Sb_2O_3$-35 $NaPO_3$-5WO_3, 60 Sb_2O_3-25 $NaPO_3$-15WO_3 systems The results show that the values are of the same order and low as a good resistance to deviation, since the glass containing 15 WO3 (% mol) is the most stable which gives a lower value of the activation energy so Chen and Ozawa methods are in good agreement and low activation energy, and there is an empirical correlation between the apparent activation energy and the stability, the results obtained by the partial recovery of the crystallization peaks are represented in Tables 3,4. The results obtained from the numerical values of the Avrami coefficient and the correlation factor >0.99 obtained are shown in Figures (5, 6, 7).

Table 3: Numerical data used to determine the Avrami coefficient by the pseudo-isothermal method for SN5W glass

α (k/min)	Ln(α)	T=451,98 x ln(-ln(1-x))	T=452,22 x ln(-ln(1-x))	T=453,14 x ln(-ln(1-x))	T=454,17 x ln(-ln(1-x))
5	1,609	0,925 0,952	0,929 0,971	0,932 0,989	0,931 0.984
8	2,079	0,882 0,759	0,887 0,779	0,898 0,825	0,908 0,872
10	2,302	0,595 -0,101	0,607 -0,069	0,641 0,024	0,674 0,115
15	2,708	0,38 -0.735	0,412 -0,633	0,442 -0,538	0,499 -0,368
20	2,996	0,1 -2,25	0,12 -2,054	0,143 -1,868	0,191 -1,55
N	----	2,26 ±0,468	2,13 ±0,435	2,02±0,414	1,79±0,376
n_{moy}	----	2,05±0,423			

Table 4: Numerical data used to determine the Avrami coefficient by the pseudo-isothermal method for SN15W glass

α (k/min)	Ln(α)	T=453,10 x ln(-ln(1-x))	T=454,53 x ln(-ln(1-x))	T=455,14 x ln(-ln(1-x))	T=456,12 x ln(-ln(1-x))
6	1,979	0,706 0,202	0,737 0,289	0,748 0,321	0,767 0,376
8	2,079	0,467 -0,463	0,525 -0,295	0,542 -0,247	0,568 -0,175
10	2,302	0,18 -1,617	0,228 -1,352	0,249 -1,251	0,289 -1,076
12	2,485	0,305 -1,011	0,352 -0,835	0,368 -0,779	0,413 -0,629
N	----	2,17±1	2±0,884	1,94±0,828	1,77±0,769
n_{moy}	----	1,97±0,870			

Then an represent Ln (-Ln(1-x)) as a function of Ln(α) . The slope of this line gives us the value of the coefficient of Avrami n.

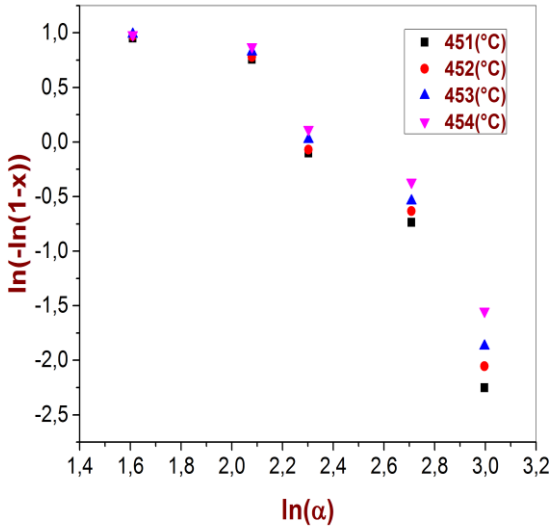

Figure 5. Determination of the coefficient of Avrami n by the isothermal pesudo method of $60Sb_2O_3$-35 $NaPO_3$-5WO_3glas

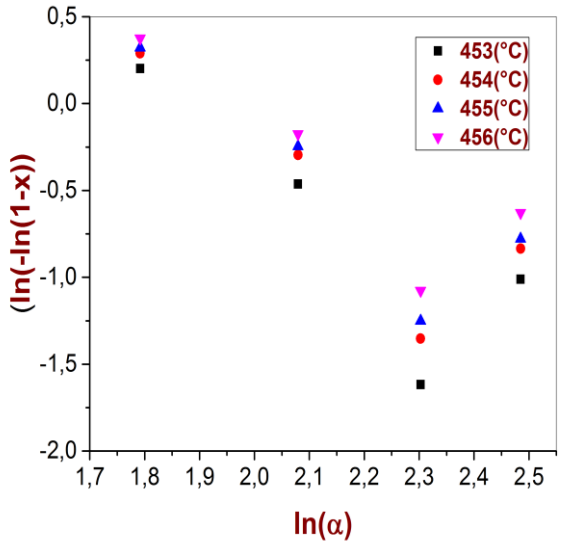

Figure 6. Determination of the coefficient of Avrami n by the isothermal pesudo method for $60Sb_2O_3$-25 $NaPO_3$-15WO_3 glass.

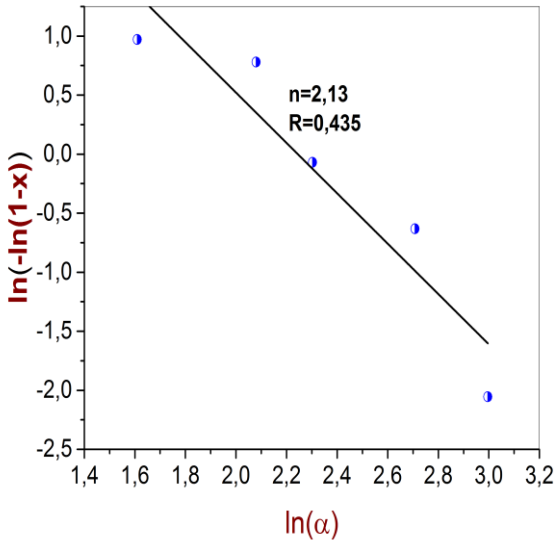

Figure 7. Determination of the Avrami n coefficient by the isothermal pesudo method of SN5W glass (T = 452).

According to the Relation between the Avrami coefficient and the nucleation rate (table 5) in a three dimensional growth controlled by the liquid/crystal interface and by diffusion it is possible to deduce the growth mechanism of the crystallisation sprouts, the glasses that have more concentration of WO3> 15% are very prone to crystallization due to the sharing corner octahedra [14].

n_{moy}= 2.05 for glass $60Sb_2O_3$-35 $NaPO_3$-5WO_3 Nucleation rate decreasing.
n_{moy}= 2.01 for glass $60Sb_2O_3$-25$NaPO_3$-15WO_3Nucleation rate decreasing.

According to the Relation between the Avrami coefficient and the nucleation rate in a three-dimensional growth. Wherever the Crystal growth controlled by diffusion n> 2,5 the nucleation rate is crescent, n=2,5 it is constant, n=1,5 it is null and 1,5 <n< 2,5 the nucleation rate is decreasing [15].

3.4. Vickers hardness (Duramin struers)

The principle consists in applying a force to the polished and the flat surface of a sample. To characterize the hardness and the deformation mode of the glass surface, the indentation technique was used. The deformation of the surface depends on the retention time of the Vickers indenture on the glass surface, on the temperature and on the applied load, and the hardness of the material can then be calculated from the projected surface of the impression [16]. The figure 8 shows the evaluation of hardness in the $60Sb_2O_3$ (40-x) $NaPO_3$-xWO_3 system glass.

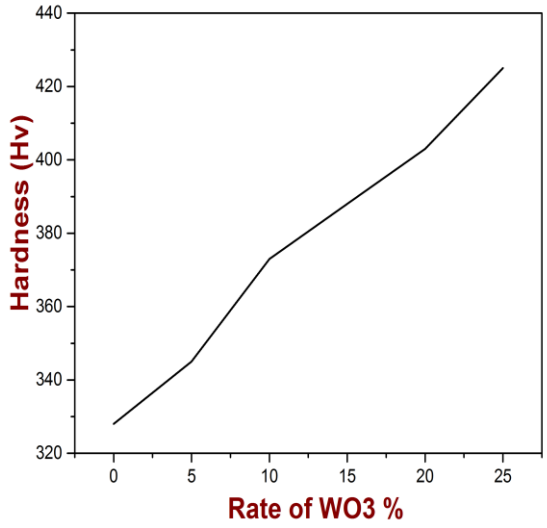

Figure 8. Hardness spectra of the $60Sb_2O_3$(40-x) $NaPO_3$-xWO_3 glass.

Hardness is the merit of surface to endure indentations, Surface hardness is related to concentrations of glasses composition in this system the Hardness increases with increasing tungsten concentration also it depend on polishing procedures that can result in increased surface hardness effect compressive strength and flexural strength [17].

4. Conclusion

The purposes of the study are to investigate Crystallization kinetics in a new ternary system Sb_2O_3-$NaPO_3$-WO_3, the parameters of crystallization have been evaluated using different methods for non-isothermal experiments, the incorporation of WO_3 produces in an apparent increase for crystallization, it improves the thermal stability of the lenses against deflection, which corresponds to the high values of the glass hardness.

Acknowledgment

The authors of this study express their gratitude to the university of Biskra Algeria for providing its lab equipment for glasses studies.

Reference

[1]. M. Nouadji, A. Attaf, R. El Abdi, M. Poulain, Journal of Alloys and Compounds. 511 (2012) 209–214.

[2]. M. T. Soltani, A. Boutarfaia, R. Makhloufi, M. Poulain, Journal of Physics and Chemistry of Solids. 64 (2003) 2307-2312.

[3]. H. Souissi, O. Taktak, O. Maalej and S. Kammoun, Journal of New Technology and Materials. 06 (2016)34-41

[4]. M. Nouadji, Z.G. Ivanova, M. Poulain, J. Zavadil, A. Attaf, Journal of Alloys and Compounds 549, 158-162 (2013).

[5]. D. Souri, , The European Physical Journal B 84.1 (2011) 47-51.

[6]. A.E. Ersundu, M. Celikbilek, M. Baazouzi, M.T. Soltani, J. Troles, S. Aydin, Journal of Alloys and Compounds, Elsevier. 615 (2014) 712 - 718.

[7]. M. T. Soltani, M.Hamzaoui, S. Houhou, , H.Touiri, L.Bediar, A. M. Ghemri, , P. Petkova, Acta Phys. Pol. A. 123 (2013) 227-229.

[8]. K. A. Aly, A. Dahshan, Y.B. Saddeek, J Therm Anal Calorim .100 (2010) 543–549.

[9]. M. Ç. Ersundu, A.E. Ersundu, M.T. Soltani, M.Baazouzi, Ceramics International. 09 (2016) 184.

[10]. O.C.L.Mocioiu, M. Zaharescu, I. Atkinson, A.M.Mocioiu, P. Budrugeac, J Therm Anal Calorim. 117 (2014) 131-139.

[11]. J. Massera, M. Mayran, J. Rocherulle, L. Hupa, J Materials Science. 50 (2015) 3091-3102.

[12]. L. Dimesso, G. Gnappi, A. Montenero, J Materials Science. 26 (1991) 4215-4219.

[13]. Y.K.Lee, S.Y.CHOI, Controlled nucleation and crystallization in Fe2O3–CaO–SiO2 glass, J Materials Science. 54 (1997) 431-436.

[14]. M. A. Abdel-Rahim, M. M. Ibrahim, M. Dongol, A. Gaber, Differential scanning calorimetric study of $Bi_{10}Se_{80}In_{10}$ chalcogenide glass, J Materials Science. 27 (1992) 4685-4689.

[15]. K.J.Rao, Structural Chemistry of Glasses, vol 125, Elsevier, 2002.

[16]. V.A.Mukhanov, O.O.Kurakevych, V.L. Solozhenko, Thermodynamic Aspects of Materials Hardness: Prediction of Novel Super Hard High Pressure Phases, High Press. Res, (2008) 1–7.

[17]. D.Venturini, MS.Cenci, FF.Demarco, GB. Camacho, Powers JM. 31 (2006) 11–17.